ACS APPLIED NANO MATERIALS
Cite This: ACS Appl. Nano Mater. XXXX, XXX, XXX−XXX
Article
www.acsanm.org

# In-Place Printing of Carbon Nanotube Transistors at Low Temperature

Jorge A. Cardenas,[†] Matthew J. Catenacci,[‡] Joseph B. Andrews,[†] Nicholas X. Williams,[†] Benjamin J. Wiley,[‡] and Aaron D. Franklin*[,†,‡]

[†]Department of Electrical and Computer Engineering and [‡]Department of Chemistry, Duke University, Durham, North Carolina 27708, United States

Supporting Information

**ABSTRACT:** Interest in flexible, stretchable, and wearable electronics has motivated the development of additive printing to fabricate customizable devices and systems directly onto virtually any surface. However, progress has been limited by the relatively high temperatures (>200 °C) required to sinter metallic inks and time-consuming process steps, many of which require removal of the substrate from the printer for coating, washing, or sintering. In this work, we addressed these challenges and demonstrate carbon nanotube thin-film transistors (CNT-TFTs) that are fabricated by aerosol jet printing with the substrate never leaving the printer. The full in-place printing approach, from first step to last, used a maximum process temperature of only 80 °C on the printer platen. Silver nanowire (Ag NW) ink was found to be most viable for low-temperature, in-place sintering while still yielding good electrical interfaces to the CNT thin-film channels. These aerosol-jet printed Ag NW films were conductive immediately after fabrication, which is the key component enabling rapid and sequential in-place printing. The devices exhibit on-currents as high as 80 μA/mm, effective mobilities of 12 $cm^2/(V{\cdot}s)$, and on/off current ratios exceeding $10^5$. These findings provide a promising path forward toward the additive manufacture of flexible and stretchable electronics in a low-cost, highly customizable, and agile manner.

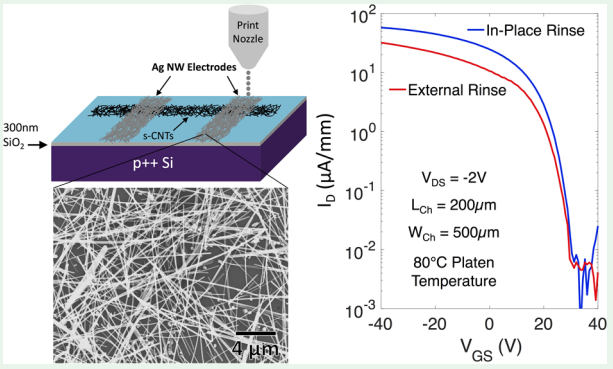


**KEYWORDS:** *carbon nanotubes (CNT), thin-film transistors (TFT), low temperature printing, silver nanowires, additive printing*

## INTRODUCTION

Printing electronics is a promising path for enabling low-cost and large-area fabrication[1] with the versatility of integrating electronics in an additive fashion[2]—directly onto virtually any surface including those that are flexible, stretchable, or porous.[3−5] In contrast to template-based printing, such as gravure or screen printing, additive (or direct-write) printing involves directly patterning functional electronic inks onto a surface without the use of a mask or other patterning steps.[6,7] Additive printing platforms, which include the inkjet and aerosol jet, are well suited for rapid prototyping, adding function directly to existing surfaces, and other low to medium throughput production environments where customization and agility are needed.[8] The inks that accompany additive printers span a wide range of material properties and electronic functionalities. For instance, organic-based inks have experienced the widest range of use, which span across printed semiconducting, conducting, and dielectric layers, owing to their high solution dispersion stability and relatively low cost.[9,10] However, the use of organic-based inks in printed electronics is hindered by unfavorable properties, such as low conductivity,[11] low carrier mobility,[12] and poor air stability.[13] More recently, inorganic inks have partly rectified these insufficiencies by offering superb electronic properties along with greater environmental and long-term performance stability.[11] Many of the prominent inorganic inks, however, such as metallic nanoparticle inks, require additional thermal and/or chemical postprocess treatments that significantly increases the time and costs associated with fabrication.[14]

While the high-temperature limitations of conductive inorganic inks persist, inorganic semiconducting carbon nanotube (s-CNT) inks have been extensively developed and lend themselves to low-temperature additive printing.[15] The randomly oriented thin-film networks that are printed from s-CNT inks require minimal thermal processing and are inherently malleable, which has enabled the demonstration of flexible and stretchable CNT-based active devices.[16−21] Carbon nanotube thin-film transistors (CNT-TFTs), specifically, have shown promise for stretchable and flexible devices suitable for many potential applications, including environmental sensors,[22,23] biosensors,[24,25] wearable electronics,[26] and many more.[27−29] A major obstacle for all types of high mobility (>1 $cm^2/(V\ s)$) printed CNT-TFTs reported to date is that their fabrication requires processing that is external from the

Received: February 16, 2018
Accepted: April 6, 2018
Published: April 6, 2018




DOI: 10.1021/acsanm.8b00269
ACS Appl. Nano Mater. XXXX, XXX, XXX−XXX

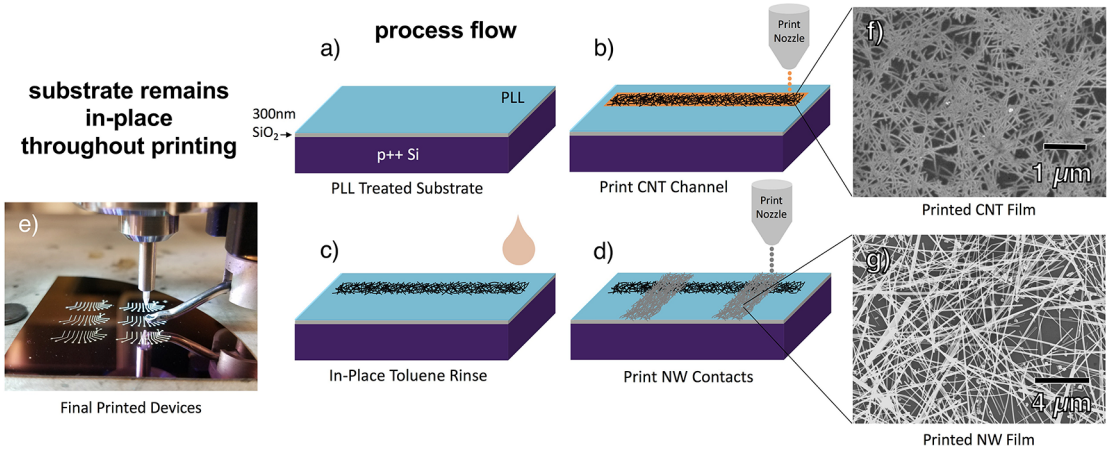


**Figure 1.** In-place printing of CNT-TFTs. (a) Prior to printing, the $Si/SiO_2$ substrate is cleaned with acetone, IPA, DI water, and $O_2$ plasma and then functionalized with poly-L-lysine and loaded into the printer; (b) an s-CNT thin-film channel is printed; (c) residual surfactant is removed from the s-CNT film using an in-place toluene rinse; and (d) Ag NW source/drain electrodes are printed. No thermal postprocessing is required. (e) Optical image of final CNT-TFTs after NW printing. SEM images of printed (f) s-CNT and (g) Ag NW thin films.

printer. Few CNT-based inks compatible with roll-to-roll (template-based) printing do not require external processing; however, these inks consist of a polymer binder matrix that severely compromises performance.[4,30] For higher performance and additive (direct-write) printing methods, CNT films require solvent rinsing after printing,[31,32] which is traditionally carried out external from a printer. However, a truly additive printing process requires that no additional processing is needed outside of the printer, so that electronics can literally be added to any arbitrary surface, regardless of its size or structure. This would require metallic contacts that are immediately conductive after printing with no additional thermal post-processing. Such demonstrations have only been accomplished using metallic-CNT contacts that are highly resistive[12,32] and conductive polymer contacts that are both resistive and environmentally unstable.[33]

One encouraging path for low-temperature printed contacts is with silver nanowires (Ag NWs). Recent studies have shown that high aspect ratio Ag NW networks dried at 70 °C are more conductive than Ag nanoparticle (Ag NP) networks dried at 200 °C.[34] Few studies in the printed electronics space have taken advantage of the low-temperature properties of Ag NWs and those that do are limited by their printing approach. For instance, nozzle clogging has limited the length of the NWs that can be deposited by an inkjet printer[35] and ink viscosity restrictions have required high organic binder content in Ag NW screen printed pastes,[36] both of which necessitate the use of elevated postprocess temperatures to obtain conductive films. Aerosol jet printers, however, may be the most suitable printing platform for patterning Ag NW inks for two reasons. First, the NWs will not require length trimming due to the fact that aerosolized ink does not come into contact with the nozzle sidewalls during the aerosol jet deposition process. Second, aerosol jet atomizers are compatible with a wide range of ink properties,[37] including low viscosity inks, which reduces the fraction of organic additives that needs to be incorporated in the ink.

In this work, we demonstrate a low-temperature and in-place aerosol jet printing approach to fabricating CNT-TFTs with Ag NW contacts. The devices are fabricated entirely in-place, from first step to last, without removal of the substrate from the printer; hence, no external baking, coating, or other treatments are used once the substrate is loaded into the printer. A key component enabling in-place printing is the use of high aspect ratio Ag NW contacts, as opposed to traditional Ag NP contacts, yielding both high conductivity and low contact resistance to s-CNTs without the use of high-temperature baking steps. In addition to our demonstration of the in-place printing of CNT-TFTs, this work also presents the first use of aerosol jet printed Ag NW thin films, including the ink formulation and optimization of printing parameters for high conductivity films. Our devices, which use a maximum process temperature of 80 °C, exhibit similar, if not greater, performance when compared against printed CNT-TFTs with traditional printed contact materials and methods, indicating the utility and promise of Ag NW contacts and the in-place printing approach.

## RESULTS AND DISCUSSION

To fabricate in-place printed CNT-TFTs, p++ Si wafers with 300 nm $SiO_2$ top layers were used as substrates. The boron-doped Si substrate serves as the conductive back-gate with the 300 nm $SiO_2$ as the gate dielectric. The substrates are prepared by first cleaning in acetone, IPA, and DI water. They are then exposed to an $O_2$ plasma to remove molecular contaminates from the surface and promote CNT adhesion. The surface of the substrate is then soaked in a monomer (poly-L-lysine, 0.1 wt % in $H_2O$) to functionalize the surface to further promote CNT adhesion and film uniformity on the hydrophobic $SiO_2$ surface. From this point, the substrate can be loaded onto the printer platen and is not removed until the devices are fully printed and ready to test.

The printing process is illustrated in Figure 1. With the platen (supporting the substrate) set to 80 °C, an s-CNT film is printed with an ultrasonically atomized aerosol jet, as depicted in Figure 1b. The s-CNT layer is printed from a commercial ink consisting of 99.9% pure semiconducting nanotubes wrapped in a proprietary surfactant and dispersed in toluene (IsoSol-S100, Nanointegris Inc.). To remove the surfactant from the CNT film after printing, the substrate is rinsed with toluene directly on the platen, without removal from the printer (Figure 1c). Traditionally, this rinse step is carried out for 20−30 s external from the printer under a fume hood, followed by an additional water/IPA rinse, and finally dried using an $N_2$ gun. It is found


DOI: 10.1021/acsanm.8b00269
ACS Appl. Nano Mater. XXXX, XXX, XXX−XXX

in this work that a brief toluene rinse and $N_2$ drying step carried out directly on the heated platen leads to sufficient surfactant removal. Analysis of this rinse step is further expounded upon in later sections. Once the surfactant from the s-CNT film has been removed, the Ag NW contacts are then sequentially printed onto the channel with no additional thermal postprocessing required, as depicted in Figure 1d. The sample is then immediately ready for electrical testing. A short video of this rapid and sequential print process can be found in the Supporting Information (Supplementary Video 1).

All printing in this work was carried out using an Optomec AJ300 aerosol jet printer. The aerosol jet deposition process consists of atomizing ink into an aerosol either ultrasonically or pneumatically. Once the aerosol is generated, an inert $N_2$ carrier gas flow is used to carry the ink toward a deposition nozzle where it is focused using a secondary annular $N_2$ sheath flow, which prevents the aerosol droplets from coming into contact with the nozzle side walls. This process simultaneously focuses the aerosol gas stream down to the substrate and prevents nozzle clogging. This aerodynamic focusing at the nozzle allows for the high-resolution deposition of colloidal suspensions with feature sizes down to 10 $\mu$m when using an optimized ink. The aerosol jet deposition process is illustrated in Figure S1 in the Supporting Information. When printing CNTs, NWs, and other high aspect ratio nanoparticle inks, aerosol jet printing is advantageous due to its resilience against nozzle clogging—an issue that plagues inkjet printers. Furthermore, the wide range of inks that are compatible with aerosol jet atomizers allows for flexible ink formulation.

A key enabling aspect of the in-place printed CNT-TFTs was the realization of a printed contact metal with sufficiently high conductivity, low contact resistance to s-CNTs, and ability to be processed without sintering. The Ag NW ink developed in this study was prepared by synthesizing Ag NWs according to the polyol method[34] with wires having average lengths and diameters of 25 $\mu$m and 150 nm, respectively. The wires were then dispersed into a variety of solvents, at a concentration of 4 mg/mL, to study the impact of print process parameters on different suspensions. Using the pneumatic atomizer, it was determined that both water- and isopropanol-based solvents resulted in sufficient atomization; however, the printed lines from water-based inks exhibited poor film uniformity due to an excessive "coffee ring effect." The printed lines from isopropanol-based inks exhibited much better film uniformity but suffered from excessive overspray, large line width, and high resistivity (see optical images in Figure 2b).

To circumvent these trade-offs between water- and isopropanol-based inks, it was found that the addition of 15% ethylene glycol (EG) by volume to the isopropanol-based ink resulted in a reduction in film overspray, line width (as seen in Figure 2c), and resistivity, producing films with $R_{Sh}$ as low as 3.5 Ω/sq when printing at platen temperatures as low as 70 °C. The effect that the addition of EG had on the films printed from isopropanol-based NW inks is summarized in Figure 2. The addition of EG results in slight nonuniformities of the printed lines, and this effect is exacerbated when printing over a CNT film (see SEM images in Figure S2) owing to the considerable hydrophobicity of the CNTs. Despite this, the high aspect ratio of the NWs ensures no electrical discontinuities are present in the printed lines, and the resulting TFTs maintain high electrical performance.

Another critical development for in-place printed CNT-TFTs was to establish a sufficient rinse/bake procedure for the

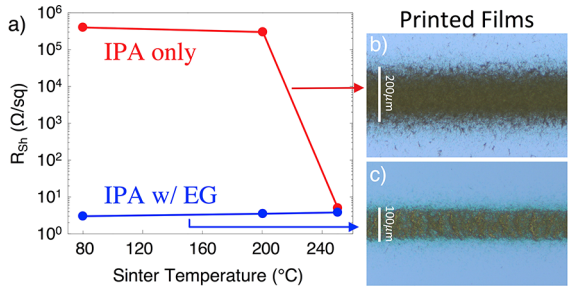


**Figure 2.** Development of low-temperature Ag NW ink. (a) Comparison of sheet resistance ($R_{Sh}$) versus sintering temperature for Ag NW films from isopropanol-based inks with (blue) or without (red) EG. (b) Optical image of isopropanol-based NW film showing excessive overspray, large line width, and high resistivity. In contrast, (c) optical image of printed NW film from ink with addition of 15% v/v EG results in improved line definition and low-temperature conductivity.

printed s-CNT thin films. To evaluate the effect of an in-place toluene rinse on CNT-TFTs, three samples were prepared and printed using either no toluene rinse, an external toluene rinse, or an in-place toluene rinse. The devices with no toluene rinse exhibited noise-level drain current ($I_d$) with no indication of current modulation as the gate voltage was swept from 40 to −40 V, indicating that without the toluene rinse electrical contact to the CNT film could not be realized. Representative subthreshold and transfer characteristics of CNT-TFTs rinsed externally (red) and in-place (blue) are provided in Figure 3,

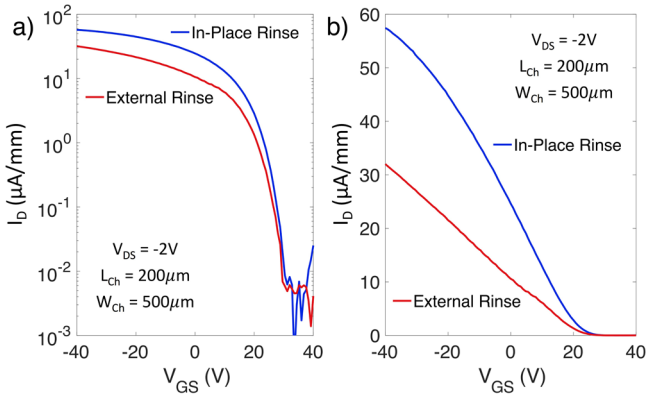


**Figure 3.** Performance comparison of in-place and traditionally printed CNT-TFTs. Representative (a) subthreshold and (b) transfer characteristics of in-place (blue) vs externally rinsed (red) CNT-TFTs. The in-place rinsed devices exhibit higher on-current and trans-conductance, with a lower subthreshold swing.

with a more comprehensive comparison between sets of externally and in-place rinsed devices in Figure S3. It can be seen that, on average, the in-place rinsed devices exhibit higher on-currents and are more uniform across sets of devices on the substrate. This is attributed to the thermal energy supplied by the 80 °C platen during the in-place rinse, which aids in surfactant removal from the CNT film. It was determined from this set of experiments that the duration of the toluene rinse needs to be no longer than a few seconds. Additionally, Raman spectroscopy measurements were carried out to verify the efficiency of the rinsing process on in-place rinsed samples (at 80 °C) and externally rinsed samples (at 20 °C), which can be seen in Figure S5. It can be seen that the radial breathing mode


DOI: 10.1021/acsanm.8b00269
ACS Appl. Nano Mater. XXXX, XXX, XXX−XXX

(RBM) peaks (100 to 200/cm range) for the in-place printed samples is much greater than that of the externally rinsed samples, indicating that the in-place rinsed samples have a cleaner surface with less organics present near the CNTs to attenuate their RBM response. The additional thermal energy supplied by the heated platen, combined with the rinsing, aids in driving off these organics, giving a much stronger RBM signal.

It was found that the in-place printed devices exhibited on/off current ratios exceeding $10^5$ and on-currents as high as 80 $\mu$A/mm. More comprehensive electrical characterization can be found in Figure 4a,b, where $I_D-V_{GS}$ curves are plotted with

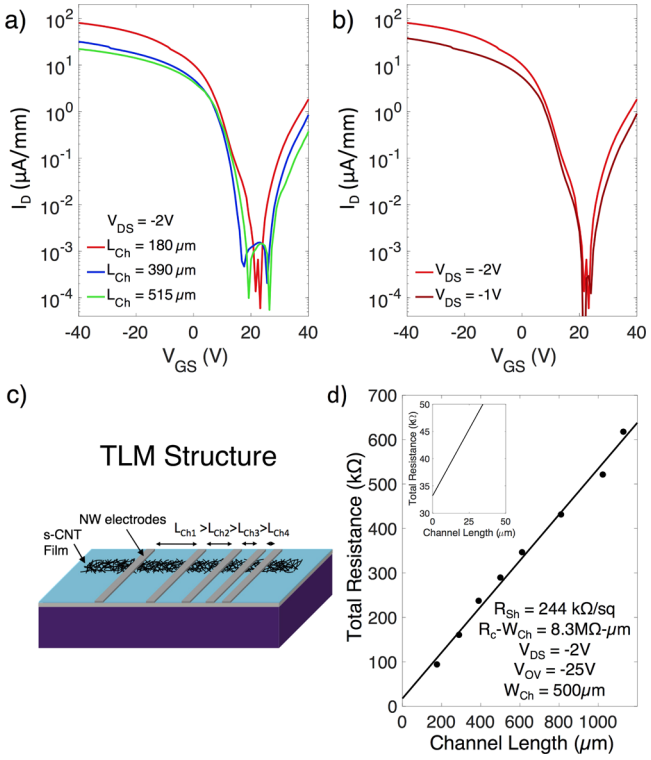


**Figure 4.** Electrical characterization of in-place printed CNT-TFTs and analysis of contact performance. Subthreshold characteristics of in-place printed CNT-TFTs with varying (a) channel lengths and (b) drain bias. (c) Schematic representation of TLM structure used to extract sheet resistance of CNT thin-film channel and contact resistance between Ag NW electrodes and the CNTs. (d) TLM plot of the total CNT-TFT resistance as a function of channel length at a constant overdrive ($V_{OV}$ = −25 V) and drain voltage ($V_{DS}$ = −2 V).

varying channel lengths and drain voltages. As anticipated for CNT-TFTs that rely on percolation transport through a channel that is exposed to ambient conditions, the devices exhibit relatively large hysteresis (see Figure S4), and the ambipolar behavior of the devices increases as the channel length decreases. The field-effect mobility extracted from these device curves is 12.25 ± 1 cm$^2$/(V s) and is calculated from the following expression: $\mu = (L_{Ch}g_m)/(W_{Ch}C_{ox}V_{DS})$, where $L_{Ch}$ and $W_{Ch}$ are the device channel length and width, respectively, $g_m$ is the peak transconductance, $V_{DS}$ = −2 V, and $C_{ox}$ is the gate capacitance per unit area as calculated using a modified parallel plate model ($C_{ox} = \varepsilon_o\varepsilon_{ox}/t_{ox} = 1.07 \cdot 10^{-8}$ F/cm$^2$) discussed in previous work.[32] An on/off ratio of $10^{5.8}$ was extracted from the shortest channel length device ($L_{Ch}$ = 180 $\mu$m). Additional information regarding device output characteristics and device-to-device variation can be found in Figure S7. To evaluate the performance of the NW contacts, the transfer length model (TLM) is used, where arrays of adjacent TFTs are printed with varying channel length ($L_{Ch}$), as illustrated in Figure 4c. The TLM structures used in this work consist of 8 CNT-TFTs with $L_{Ch}$ ranging from 180 to 1100 $\mu$m. With the use of an overdrive voltage (gate voltage minus threshold voltage) $V_{OV} = V_{GS} - V_t$ = −25 V and drain voltage $V_{DS}$ = −2 V, the device resistance is plotted against channel length (see TLM plot in Figure 4d) to extrapolate the CNT film sheet resistance ($R_{Sh}$) and the contact resistance ($R_c$). It is found that for a CNT sheet resistance of 244 kΩ/sq and an Ag NW sheet resistance of 3.5 Ω/sq, the NW-CNT contact resistance is 8.3 MΩ•$\mu$m, which is only slightly higher than the best contact resistance values from printed Ag NP contacts in the literature.[32,38] It should be noted that this contact resistance did not change when annealing the devices at temperatures as high as 200 °C.

A more comprehensive comparison between in-place printed CNT-TFTs and other CNT-TFTs from the literature is presented in Figure 5. The large, width-normalized on-currents

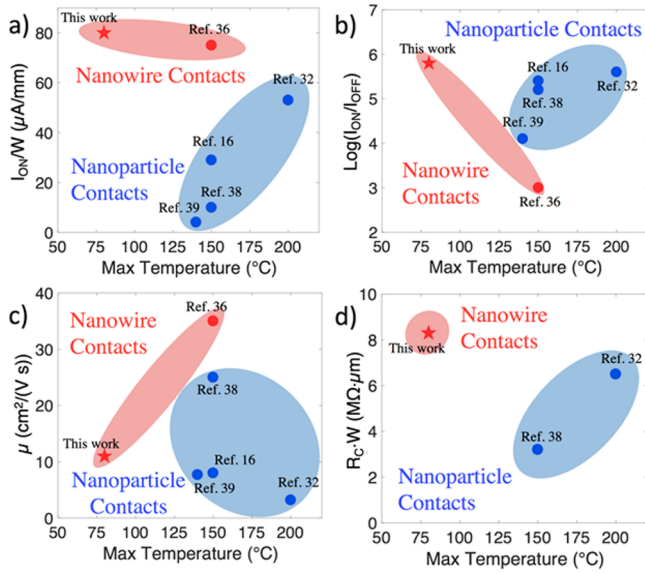


**Figure 5.** Benchmarking performance of in-place printed CNT-TFTs with other printed CNT-TFTs from literature. Comparison between maximum sintering temperatures and (a) width-normalized on-current, (b) on/off current ratio, (c) effective device mobility, and (d) width-normalized contact resistance from printed CNT-TFTs with Ag-based contacts. The red star in each plot represents the in-place printed CNT-TFTs from this work with Ag NW contacts processed at a maximum temperature of 80 °C.

reported in this work (as seen in Figure 5a) result from a combination of high s-CNT channel density, low contact resistance, and high relative overdrive voltage. As seen in Figure 5b, the devices reported in this work have a high on/off ratio that is slightly larger in comparison to on/off ratios reported from CNT-TFTs in the relevant literature.[16,32,38,39] This is attributed to an optimized CNT film density, intermediate channel lengths ($L_{Ch}$ = 180 $\mu$m), and reasonably low electrode overspray, all of which help to minimize the CNT-TFT off-current. The devices from this work exhibit intermediately high mobility values; however, the higher mobilities reported in other works are achieved through exceedingly high CNT film


DOI: 10.1021/acsanm.8b00269
ACS Appl. Nano Mater. XXXX, XXX, XXX−XXX

densities, which simultaneously lowers the on/off ratio (e.g., see reference [36] in Figures 5b,c). Finally, contact resistance values are compared in Figure 5d, where it can be seen that the devices in this work have a slightly higher contact resistance when compared to devices with printed Ag NP contacts. While contact resistance plays a comparatively small role in overall device performance compared to CNT channel resistance, $R_c$ associated with Ag NW-CNT interfaces can be improved with higher NW film densities. Overall, we show here that high device performance is achieved in CNT-TFTs with Ag NW contacts without using temperatures above 80 °C and without physically removing the substrate from the printer.

## CONCLUSION

In summary, we have shown that CNT-TFTs with Ag NW contacts can be printed in-place and in an additive fashion without the use of high-temperature processing steps. This rapid and sequential printing process makes use of an in-place toluene rinse on the printed CNT channel, which aids in surfactant removal and boosts the resulting device performance. Meanwhile, it was shown that the addition of EG to an isopropanol-based Ag NW ink results in highly conductive films when dried at low temperatures, enabling a CNT-TFT contact material with low contact resistance, even when processed at temperatures as low as 80 °C. The in-place printed CNT-TFTs fabricated in this work exhibit device performance comparable to the best printed CNT-TFTs in the literature while using far fewer process steps and much lower process temperatures. While in-place printing of the s-CNT channel and conductive electrodes is a substantial first step along the path to low-cost, additively printed CNT-TFT technologies, a significant obstacle moving forward will be the development of a dielectric ink that is also compatible with in-place printing. A variety of dielectric inks have been demonstrated using additive printers, and the challenge will be to identify which materials are most compatible with low-temperature and in-place processing while remaining stable, thin, and pinhole free. The findings in this work address challenges associated with additive printing in a CNT-TFT print process that is rapid, agile, low-cost, and suitable for the further development of emerging applications such as flexible, stretchable, and biointegrated electronics.

## METHODS

**Substrate Cleaning.** The Si substrates were rinsed with DI water and then ultrasonicated in acetone and IPA for 5 min each. The wafers were then rinsed again using DI water and dried using an $N_2$ gun. Finally, the wafers were subjected to 4 min of an $O_2$ plasma (Emitech K-1050X) at 100W under low vacuum (0.6 Torr).

**Wafer Functionalization.** Prior to printing the CNT channel, the wafers are soaked in a poly-L-lysine (0.1% w/v in water; Sigma-Aldrich) bath for 5 min to promote CNT adhesion. Excess monomer is then rinsed off the wafer with DI water. Finally, the wafer is dried thoroughly using an $N_2$ gun.

**Printing CNT Channels.** The high purity (>99.9%) single walled semiconducting CNT ink (IsoSol-S100) was purchased from Nano-integris, Inc., Canada at a CNT concentration of 0.05 mg/mL. It was then further diluted with toluene to a concentration of 0.01 mg/mL for ultrasonic atomization. After dilution, the CNT ink was ultrasonicated for 30 min to eliminate the aggregation of CNTs that form during the dilution process. Then, 2 mL of the ink was then loaded into the ultrasonic atomizer for aerosol jet printing (Optomec, Inc.). The ink was then printed using a 150 $\mu$m nozzle, a sheath gas flow rate of 40 sccm, a carrier gas flow rate of 23 sccm, and an ultrasonic transducer current of 330 mA. The water bath on the ultrasonic atomizer was kept at room temperature, while the printer platen was set at 80 °C. The CNT films were printed at a speed of 1 mm/s using two print passes to achieve a sufficiently dense film for maximizing the device on/off ratio. All print parameters used for printing the CNT ink have been developed and optimized in previous work, as described in reference [32]. The resulting CNT films have a mean thickness of 9 nm with an RMS surface roughness of 3 nm (see AFM image in Figure S6).

**In-Place Rinsing.** During solvent rinsing, the sample remains flat on the 80 °C platen through the use of a platen vacuum. A squirt bottle is used to deposit toluene on the surface of the sample. The duration of the toluene rinse needs to be no longer than a few seconds. After deposition, the excess toluene is blown off the surface of the sample using a $N_2$ gun. The excess toluene that remains on the heated platen quickly evaporates. This process can be seen in real time in Supplementary Video 1.

**Ag NW Ink and Printing.** The high aspect ratio Ag NWs in this study were synthesized according to the polyol method as described in reference [34]. The wires were then rinsed and dispersed into isopropanol at a concentration of 4 mg/mL. Next, 15% v/v EG was added to the IPA/NW solution and mixed in a vortexer for 1 min. Then, 15−20 mL of ink was loaded into the pneumatic atomizer of an aerosol jet printer (Optomec, Inc.). With the pneumatic atomizer kept at room temperature and the platen kept at 80 °C, the Ag NW electrodes were then printed directly over the CNT channels using a nozzle diameter of 300 $\mu$m, a sheath gas flow rate of 45 sccm, an atomizer flow rate of 280 sccm, and an exhaust flow rate of 260 sccm. Printed films had a $R_{Sh}$ = 3.5Ω/sq when using three print passes and a print speed of 1 mm/s. Printed line widths were measured to be 80−100 $\mu$m. Line thicknesses were measured using a profilometer to be approximately 1 $\mu$m.

**Characterization of Printed Devices.** Optical images of printed devices were taken using a Zeiss Axio Lab microscope with 2.5 to 100× objective lenses while using a digital camera for image capture. SEM images of printed patterns and devices were acquired using a FEI XL30 (SEM-FEG). Electrical characterization was carried out in air using a table top probe station and a Lakeshore vacuum probe station (Lakeshore CRX-6.5K) along with a B1500A Device Analyzer (Keysight Technologies). The sheet resistance measurements were carried out using a four-point probe method and a Keithley 2400 source measure unit. Raman spectroscopy measurements were taken using a Horiba Jobin Yvon LabRam ARAMIS using a 633 nm laser excitation. AFM measurements were taken using a Digital Instruments Dimension 3100 on tapping mode. Profilometry measurements were carried out using a Bruker Dektak 150.

## ASSOCIATED CONTENT

### Supporting Information

The Supporting Information is available free of charge on the ACS Publications website at DOI: 10.1021/acsanm.8b00269.

An illustration and description of the aerosol jet printing process, additional SEM images of the Ag NW films, subthreshold characteristic comparisons between in-place rinsed vs externally rinsed devices, double sweep subthreshold characteristics, Raman data for in-place rinsed devices, AFM images of CNT films, CNT-TFT output characteristics, and uniformity data on in-place printed CNT-TFTs (PDF)

Video file of the in-place printing of CNT-TFTs (MPG)

## AUTHOR INFORMATION

### Corresponding Author

*E-mail: aaron.franklin@duke.edu; Tel: +1-919-681-9471.

### ORCID

Jorge A. Cardenas: 0000-0002-4403-8962

Benjamin J. Wiley: 0000-0002-1314-6223

Aaron D. Franklin: 0000-0002-1128-9327



DOI: 10.1021/acsanm.8b00269
ACS Appl. Nano Mater. XXXX, XXX, XXX−XXX

## Notes

The authors declare the following competing financial interest(s): Author A. D. Franklin declares a financial conflict of interest with Tyrata, Inc, which uses printed carbon nanotubes for material thickness sensing applications in tires.

## ■ ACKNOWLEDGMENTS

This work was supported by the Department of Defense Congressionally Directed Medical Research Program (CDMRP) under award number W81XWH-17-2-0045. J.A.C. acknowledges support from the National Science Foundation (NSF) through the NSF graduate research fellowship (grant no. DGE 11010101-0417-7172-7172/4103). This work was performed in part at the Duke University Shared Materials Instrumentation Facility (SMIF), a member of the North Carolina Research Triangle Nanotechnology Network (RTNN), which is supported by the National Science Foundation (Grant ECCS-1542015) as part of the National Nanotechnology Coordinated Infrastructure (NNCI).

## ■ REFERENCES

(1) Parashkov, R.; Becker, E.; Riedl, T.; Johannes, H. H.; Kowalsky, W. Large Area Electronics Using Printing Methods. *Proc. IEEE* **2005**, *93*, 1321−1329.

(2) Khan, S.; Lorenzelli, L.; Dahiya, R. S. Technologies for Printing Sensors and Electronics Over Large Flexible Substrates: A Review. *IEEE Sens. J.* **2015**, *15*, 3164−3185.

(3) Rogers, J. A.; Someya, T.; Huang, Y. Materials and Mechanics for Stretchable Electronics. *Science* **2010**, *327*, 1603−1607.

(4) Chen, K.; Gao, W.; Emaminejad, S.; Kiriya, D.; Ota, H.; Nyein, H. Y. Y.; Takei, K.; Javey, A. Printed Carbon Nanotube Electronics and Sensor Systems. *Adv. Mater.* **2016**, *28*, 4397−4414.

(5) Tobjörk, D.; Österbacka, R. Paper Electronics. *Adv. Mater.* **2011**, *23*, 1935−1961.

(6) Tekin, E.; Smith, P. J.; Schubert, U. S. Inkjet Printing as a Deposition and Patterning Tool for Polymers and Inorganic Particles. *Soft Matter* **2008**, *4*, 703−713.

(7) Seifert, T.; Sowade, E.; Roscher, F.; Wiemer, M.; Gessner, T.; Baumann, R. R. Additive Manufacturing Technologies Compared: Morphology of Deposits of Silver Ink Using Inkjet and Aerosol Jet Printing. *Ind. Eng. Chem. Res.* **2015**, *54*, 769−779.

(8) King, B; Renn, M. *Aerosol Jet Direct Write Printing for Mil-Aero Electronic Applications*; Optomec: Albuquerque, NM, U.S.A., 2009; https://www.optomec.com/wp-content/uploads/2014/04/Optomec_Aerosol_Jet_Direct_Write_Printing_for_Mil_Aero_Electronic_Apps.pdf.

(9) Berggren, M.; Nilsson, D.; Robinson, N. D. Organic Materials for Printed Electronics. *Nat. Mater.* **2007**, *6*, 3−5.

(10) Chung, S.; Kim, S. O.; Kwon, S. K.; Lee, C.; Hong, Y. All-Inkjet-Printed Organic Thin-Film Transistor Inverter on Flexible Plastic Substrate. *IEEE Electron Device Lett.* **2011**, *32*, 1134−1136.

(11) Perelaer, J.; Smith, P. J.; Mager, D.; Soltman, D.; Volkman, S. K.; Subramanian, V.; Korvink, J. G.; Schubert, U. S. Printed Electronics: The Challenges Involved in Printing Devices, Interconnects, and Contacts Based on Inorganic Materials. *J. Mater. Chem.* **2010**, *20*, 8446−8453.

(12) Okimoto, H.; Takenobu, T.; Yanagi, K.; Miyata, Y.; Shimotani, H.; Kataura, H.; Iwasa, Y. Tunable Carbon Nanotube Thin-Film Transistors Produced Exclusively via Inkjet Printing. *Adv. Mater.* **2010**, *22*, 3981−3986.

(13) Beecher, P.; Servati, P.; Rozhin, A.; Colli, A.; Scardaci, V.; Pisana, S.; Hasan, T.; Flewitt, A. J.; Robertson, J.; Hsieh, G. W.; et al. Ink-Jet Printing of Carbon Nanotube Thin Film Transistors. *J. Appl. Phys.* **2007**, *102*, 043710.

(14) Rajan, K.; Roppolo, I.; Chiappone, A.; Bocchini, S.; Perrone, D.; Chiolerio, A. Silver Nanoparticle Ink Technology: State of the Art. *Nanotechnol., Sci. Appl.* **2016**, *9*, 1−13.

(15) Ding, J.; Li, Z.; Lefebvre, J.; Cheng, F.; Dunford, J. L.; Malenfant, P. R.; Humes, J.; Kroeger, J. A Hybrid Enrichment Process Combining Conjugated Polymer Extraction and Silica Gel Adsorption for High Purity Semiconducting Single-Walled Carbon Nanotubes (SWCNT). *Nanoscale* **2015**, *7*, 15741−15747.

(16) Lau, P. H.; Takei, K.; Wang, C.; Ju, Y.; Kim, J.; Yu, Z.; Takahashi, T.; Cho, G.; Javey, A. Fully Printed, High Performance Carbon Nanotube Thin-Film Transistors on Flexible Substrates. *Nano Lett.* **2013**, *13*, 3864−3869.

(17) Cao, Q.; Kim, H. S.; Pimparkar, N.; Kulkarni, J. P.; Wang, C.; Shim, M.; Roy, K.; Alam, M. A.; Rogers, J. A. Medium-Scale Carbon Nanotube Thin-Film Integrated Circuits on Flexible Plastic Substrates. *Nature* **2008**, *454*, 495−500.

(18) Chandra, B.; Park, H.; Maarouf, A.; Martyna, G. J.; Tulevski, G. S. Carbon Nanotube Thin Film Transistors on Flexible Substrates. *Appl. Phys. Lett.* **2011**, *99*, 072110.

(19) Cao, C.; Andrews, J. B.; Franklin, A. D. Completely Printed, Flexible, Stable, and Hysteresis-Free Carbon Nanotube Thin-Film Transistors via Aerosol Jet Printing. *Adv. Electron. Mater.* **2017**, *3*, 1700057.

(20) Liang, J.; Li, L.; Chen, D.; Hajagos, T.; Ren, Z.; Chou, S. Y.; Hu, W.; Pei, Q. Intrinsically Stretchable and Transparent Thin-Film Transistors Based on Printable Silver Nanowires, Carbon Nanotubes and an Elastomeric Dielectric. *Nat. Commun.* **2015**, *6*, 7647.

(21) Xu, F.; Wu, M. Y.; Safron, N. S.; Roy, S. S.; Jacobberger, R. M.; Bindl, D. J.; Seo, J. H.; Chang, T. H.; Ma, Z.; Arnold, M. S. Highly Stretchable Carbon Nanotube Transistors with Ion Gel Gate Dielectrics. *Nano Lett.* **2014**, *14*, 682−686.

(22) Zhang, H.; Xiang, L.; Yang, Y.; Xiao, M.; Han, J.; Ding, L.; Zhang, Z.; Hu, Y.; Peng, L. M. High-Performance Carbon Nanotube Complementary Electronics and Integrated Sensor Systems on Ultrathin Plastic Foil. *ACS Nano* **2018**, *12*, 2773.

(23) Andrews, J. B.; Cardenas, J. A.; Mullett, J.; Franklin, A. D. Fully Printed and Flexible Carbon Nanotube Transistors Designed for Environmental Pressure Sensing and Aimed at Smart Tire Applications. Proceedings of IEEE Sensors 2017, Glasgow, Scotland, October 30−November 1, 2017.

(24) Yamada, T.; Hayamizu, Y.; Yamamoto, Y.; Yomogida, Y.; Izadi-Najafabadi, A.; Futaba, D. N.; Hata, K. A Stretchable Carbon Nanotube Strain Sensor for Human-Motion Detection. *Nat. Nanotechnol.* **2011**, *6*, 296−301.

(25) Gruner, G. Carbon Nanotube Transistors for Biosensing Applications. *Anal. Bioanal. Chem.* **2006**, *384*, 322−335.

(26) Son, D.; Koo, J. H.; Song, J. K.; Kim, J.; Lee, M.; Shim, H. J.; Park, M.; Lee, M.; Kim, J. H.; Kim, D. H. Stretchable Carbon Nanotube Charge-Trap Floating-Gate Memory and Logic Devices for Wearable Electronics. *ACS Nano* **2015**, *9*, 5585−5593.

(27) Gaviria Rojas, W. A.; McMorrow, J. J.; Geier, M. L.; Tang, Q.; Kim, C. H.; Marks, T. J.; Hersam, M. C. Solution-Processed Carbon Nanotube True Random Number Generator. *Nano Lett.* **2017**, *17*, 4976−4981.

(28) Wang, C.; Chien, J. C.; Takei, K.; Takahashi, T.; Nah, J.; Niknejad, A. M.; Javey, A. Extremely Bendable, High-Performance Integrated Circuits Using Semiconducting Carbon Nanotube Networks for Digital, Analog, and Radio-Frequency Applications. *Nano Lett.* **2012**, *12*, 1527−1533.

(29) Geier, M. L.; McMorrow, J. J.; Xu, W.; Zhu, J.; Kim, C. H.; Marks, T. J.; Hersam, M. C. Solution-Processed Carbon Nanotube Thin-Film Complementary Static Random Access Memory. *Nat. Nanotechnol.* **2015**, *10*, 944−948.

(30) Koo, H.; Lee, W.; Choi, Y.; Sun, J.; Bak, J.; Noh, J.; Subramanian, V.; Azuma, Y.; Majima, Y.; Cho, G. Scalability of Carbon-Nanotube-Based Thin Film Transistors for Flexible Electronic Devices Manufactured Using an All Roll-to-Roll Gravure Printing System. *Sci. Rep.* **2015**, *5*, 14459.

(31) Homenick, C. M.; James, R.; Lopinski, G. P.; Dunford, J.; Sun, J.; Park, H.; Jung, Y.; Cho, G.; Malenfant, P. R. Fully Printed and Encapsulated SWCNT-Based Thin Film Transistors via a Combina-



DOI: 10.1021/acsanm.8b00269
*ACS Appl. Nano Mater.* XXXX, XXX, XXX−XXX

tion of R2R Gravure and Inkjet Printing. *ACS Appl. Mater. Interfaces* **2016**, *8*, 27900−27910.
(32) Cao, C.; Andrews, J. B.; Kumar, A.; Franklin, A. D. Improving Contact Interfaces in Fully Printed Carbon Nanotube Thin-Film Transistors. *ACS Nano* **2016**, *10*, 5221−5229.
(33) Kim, Y. H.; Lee, J.; Hofmann, S.; Gather, M. C.; Müller-Meskamp, L.; Leo, K. Achieving High Efficiency and Improved Stability in ITO-Free Transparent Organic Light-Emitting Diodes with Conductive Polymer Electrodes. *Adv. Funct. Mater.* **2013**, *23*, 3763−3769.
(34) Stewart, I. E.; Kim, M. J.; Wiley, B. J. Effect of Morphology on the Electrical Resistivity of Silver Nanostructure Films. *ACS Appl. Mater. Interfaces* **2017**, *9*, 1870−1876.
(35) Finn, D. J.; Lotya, M.; Coleman, J. N. Inkjet Printing of Silver Nanowire Networks. *ACS Appl. Mater. Interfaces* **2015**, *7*, 9254−9261.
(36) Liang, J.; Tong, K.; Pei, Q. A Water-Based Silver-Nanowire Screen-Print Ink for the Fabrication of Stretchable Conductors and Wearable Thin-Film Transistors. *Adv. Mater.* **2016**, *28*, 5986−5996.
(37) *Aerosol Jet 300 Series Datasheet*; Optomec: Albuquerque, NM, U.S.A., 2016; https://www.optomec.com/wp-content/uploads/2014/04/AJ-300-Systems-Web0417.pdf.
(38) Lee, Y.; Yoon, J.; Choi, B.; Lee, H.; Park, J.; Jeon, M.; Han, J.; Lee, J.; Kim, Y.; Kim, D. H.; et al. Semiconducting Carbon Nanotube Network Thin-Film Transistors with Enhanced Inkjet-Printed Source and Drain Contact Interfaces. *Appl. Phys. Lett.* **2017**, *111*, 173108.
(39) Cao, X.; Lau, C.; Liu, Y.; Wu, F.; Gui, H.; Liu, Q.; Ma, Y.; Wan, H.; Amer, M. R.; Zhou, C. Fully Screen-Printed, Large-Area, and Flexible Active-Matrix Electrochromic Displays Using Carbon Nanotube Thin-Film Transistors. *ACS Nano* **2016**, *10*, 9816−9822.


DOI: 10.1021/acsanm.8b00269
*ACS Appl. Nano Mater.* XXXX, XXX, XXX−XXX